

## Electrolysis of pure water in a thin layer cell

|       |   |
|-------|---|
| メタデータ | 言語: English<br>出版者:<br>公開日: 2016-03-24<br>キーワード (Ja):<br>キーワード (En):<br>作成者: Aoki, Koichi Jeremiah, Li, Chunyan, Nishiumi,<br>Toyohiko, Chen, Jingyuan<br>メールアドレス:<br>所属: |
| URL   | <a href="http://hdl.handle.net/10098/9864">http://hdl.handle.net/10098/9864</a>   |

# Electrolysis of pure water in a thin layer cell

Koichi Jeremiah Aoki<sup>\*</sup>, Chunyan Li, Toyohiko Nishiumi, Jingyuan Chen

Department of Applied Physics, University of Fukui, 3-9-1 Bunkyo, Fukui, 910-0017  
Japan

## Abstract

Current-voltage curves were obtained at parallel platinum electrodes in the thin layer cell including pure water. They were under the steady state in the voltage domain from 1.0 V to 1.3 V when the distance of the electrodes was less than 100  $\mu\text{m}$ . The solution resistance obtained from the current-voltage curve was much smaller than that predicted from the resistivity of pure water. The reason can be explained in terms of generation and accumulation of hydrogen ion and hydroxide ion before the recombination reaction. These kinetically survived ions decrease the resistance, and enhance the electrolysis rate. We subtract the reaction-controlled current-voltage curves from the overall curves to evaluate ion-included solution resistance. The resistivity of the solution averaged in the cell increased with an increase in the distance between the electrodes. In order to understand the above behavior, we calculated concentration profiles of the ions and potential distribution in the cell on the basis of Nernst-Planck equation including dissociation kinetics of water.

Key words: dissociation kinetics of water; resistivity of water; electrolysis of pure water in thin layer cell; Nernst-Planck equation

---

<sup>\*</sup> Phone +81 776 27 8665, Fax +81 776 27 8750, e-mail [kaoki@u-fukui.ac.jp](mailto:kaoki@u-fukui.ac.jp) (k.J. Aoki)

## 1. Introduction

Micro-reactors have been employed for synthesizing small amounts of unstable chemicals for immediate use [1,2]. They are suitable for reactions under conditions of uncommonly high temperature, high concentration and high purity. In addition, they can control such accurate reaction parameters as to achieve subtle mixing and localized concentration [3]. These advantages can be realized in electrochemical micro-reactors, which facilitate ionic transport due to local electric fields, interaction of products at an anode and a cathode, and occurrence of unexpected reactions with salts [4,5]. Several examples can be cited briefly in the following. Micro-electrolysis can be performed at low concentration of supporting electrolyte because of low solution resistance in a small cell [6-9]. The flow cell with a narrow electrode separation has allowed electrochemical treatments of water without supporting electrolytes [10]. Mass transport of electrochemical products to a counter electrode has been discussed in the light of optimization of cell structures [11]. Electrolysis voltage at segmented electrodes has been controlled locally to a diffusion-limited value [12]. Although reaction potential cannot be poorly controlled in conventional, synthetic cells, micro-reactors have made it possible to obtain cyclic voltammograms [13]. Microfluidic channel flow devices have been fabricated for in situ simultaneous hydrodynamic electrochemical ESR, resulting in minimal dielectric loss and a high level of sensitivity [14,15]. Generator-collector experiments in flow cells have been made at a single macroelectrode, and used to detect local pH changes adjacent to the electrode surface [16,17]. Electrochemical coupling between parallel microbands in the linear microchannel is useful for evaluating in situ the average velocity rates of the flow [18]. Recent work on electrochemical micro-reactors has been reviewed and a number of examples can be seen [19].

Conductivity of solution at low concentration of supporting electrolyte varies with an advance of reactions because reaction products have electric charge different from

the reactants. The complication has been discussed in the field of microelectrode voltammetry [20-31]. Further complication occurs at a thin layer cell, because products at the anode reach the cathode at which they react, called reaction coupling [32]. The coupling ought to enhance reaction rates, as for redox cycling at interdigitated electrodes [33-35]. Unfortunately, the coupling has not yet been discussed quantitatively, to our knowledge, not only theoretically but also by experimentally.

Our concern here is a possibility of electro-decomposition of pure water by a micro-reactor. We consider, as an example, a thin layer cell composed of two planar electrodes  $A = 1 \text{ cm}^2$  in area with the inter-distance,  $w = 10 \text{ }\mu\text{m}$ . Since the resistivity of pure water is  $18 \text{ M}\Omega \text{ cm}$  owing to the ionic concentration,  $[\text{H}^+] = [\text{OH}^-] = 10^{-7} \text{ M}$  ( $= \text{mol dm}^{-3}$ ), the resistance of the cell is  $18 \text{ k}\Omega$ . If water is electro-decomposed into hydrogen ion and hydroxide ion by the current density  $0.1 \text{ mA cm}^{-2}$ , the ohmic voltage of the solution resistance becomes  $1.8 \text{ V}$ . Then the total voltage becomes  $1.8 + 1.23$  (thermodynamic voltage)  $= 3.2 \text{ V}$ . This estimation is over-simplified, because products,  $\text{H}^+$  and  $\text{OH}^-$ , decrease solution resistance in the cell, as illustrated in Fig. 1. Then the overvoltage by the resistance can contribute to the electrolysis to enhance the current density. The current may decrease the resistance further. This virtuous circle may be used for industrious electrolysis of pure water, the alternative to the technique of solid polymer electrolyte films [36,37].

We aim at the kinetic mass transport problem of water electrolysis without supporting electrolyte in a thin layer cell. A question is whether an electric double layer required for the electrolysis is formed in pure water or not. If a double layer is generated, another question is about how thin inter-distance of the parallel electrodes and how much voltage can decompose water without supporting electrolyte. These questions will be solved experimentally by measuring current-voltage curves in a thin layer cell and theoretically by examining numerical solution of diffusion-migration equations including the reaction kinetics.

## 2. Experimental

Two platinum rods 2 mm in diameter were used for the electrode by facing their bottom surfaces each other, as are illustrated in Fig. 2. One of them was fixed horizontally, whereas the other was moved in the direction of the rod axis by means of a micrometer gauge of an optical positioner. The axis of a cylindrical rod was fitted to the axis of the other rod by a microscope. The rods were coated with a polyethylene vessel, which was a part of a bellows pipette, 5 mm<sup>3</sup> in volume. Pure water was inserted into the vessel through a hole of the top of the vessel by means of a syringe so that water overflowed. The side faces of the rods were not insulated so that they were exposed to water. The side surfaces do not contribute to the electrode reactions because distance between at any point on the side face and the bottom face of the counter rod ( $w_s$  in Fig. 2) is much larger than the distance between the two bottom faces,  $w$ . Therefore the actual working area of the electrode is 3.14 mm<sup>2</sup>. We attempted to use commercially available disk platinum electrodes coated with polyether ether ketone (PEEK). The current-voltage curves varied from electrodes and electrodes. The irreproducibility seems to be ascribed to crevice between the coating material and the platinum by gas evolution.

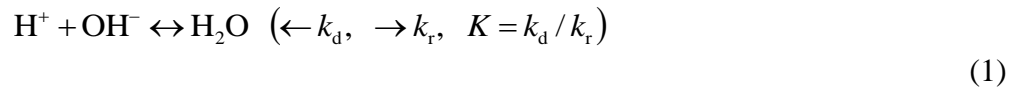
Water was prepared with an ultrapure water system, CPW-100 (Advantec, Tokyo), and was deaerated with nitrogen gas. The resistivity of the water before electrochemical measurements was 18 M $\Omega$  cm by means of the conductometer equipped with the pure water generator. The cell into which pure water was injected was set in nitrogen atmosphere. The distance between the two electrodes was the length read by the micrometer gauge from the contacting point of the two bottom surfaces. Voltage was applied to the two electrodes with a potentiostat, Compactstat (Ivium, Netherlands). A conductometer was DS-71 (Horiba, Kyoto) for pure water.

Voltammetry was made in nitrogen atmosphere covered with a plastic bag under the nitrogen gas pressure slightly larger than the atmospheric pressure at room temperature ( $24 \pm 2$  °C). The water in the cell was quiescent. Voltammograms for decomposition of water without solution resistance were obtained in  $0.1 \text{ mol dm}^{-3}$   $\text{NaClO}_4$  aqueous solution at film-coated platinum rods. Reproducibility of the voltammograms was confirmed by overlap of three times voltammograms.

### 3. Results and Discussion

#### 3.1 Computation of concentration profiles

Electrolysis of water is represented by  $2\text{H}_2\text{O} \rightarrow 2\text{H}^+ + \text{H}_2\text{O}_2 + 2\text{e}^-$  or  $2\text{H}_2\text{O} \rightarrow 4\text{H}^+ + \text{O}_2 + 4\text{e}^-$  at an anode, and  $2\text{H}_2\text{O} + 2\text{e}^- \rightarrow 2\text{OH}^- + \text{H}_2$  at a cathode. The products,  $\text{H}^+$  and  $\text{OH}^-$ , of pure water are recombined each other in the bulk through



At parallel electrodes with a very narrow inter-electrode distance,  $w$ , the product  $\text{H}^+$  at the anode reacts with the product  $\text{OH}^-$  at the cathode to reach the equilibrium. Then the redox cycle occurs to enhance the current. Conditions of causing the redox cycle may depend not only on  $w$  and  $k_r$  but also on fluxes of the ions by diffusion and electric migration. Therefore we formulate here the mass transport.

The concentrations of  $\text{H}^+$  and  $\text{OH}^-$ , denoted by  $c_+$  and  $c_-$  respectively, are satisfied with the continuum and kinetic equation for fluxes  $J_+$  of  $\text{H}^+$  and  $J_-$  of  $\text{OH}^-$

$$\frac{\partial c_{\pm}}{\partial t} + \frac{\partial J_{\pm}}{\partial x} = k_d c_{\text{H}_2\text{O}} - k_r c_+ c_- \quad (2)$$

where  $x$  is the distance from the surface of the cathode to the solution (Fig. 1). When the both ions are controlled with diffusion and electric migration for the electric potential,  $\phi$ , in the solution, their concentrations are satisfied with the Nernst-Planck equations:

$$J_{\pm} = -D \frac{\partial c_{\pm}}{\partial x} \mp \frac{F}{RT} D c_{\pm} \frac{\partial \phi}{\partial x} \quad (3)$$

where  $D$  is the diffusion coefficient common to both ions. Although the diffusion coefficient of  $H^+$  is four times larger than that of  $OH^-$ , we use this assumption in order to know approximately potential and concentration distributions in the cell rather than to fit experimental data. Elimination of  $J_{\pm}$  from eq. (2) and (3) yields

$$\frac{\partial c_{\pm}}{\partial t} = D \frac{\partial^2 c_{\pm}}{\partial x^2} \pm \frac{FD}{RT} \frac{\partial}{\partial x} \left( c_{\pm} \frac{\partial \phi}{\partial x} \right) + k_r (Kc_{H_2O} - c_+ c_-) \quad (4)$$

In contrast, the potential distribution is determined by Poisson's equation:

$$d^2 \phi / dx^2 = -F(c_+ - c_-) / \varepsilon_0 \varepsilon_r \quad (5)$$

where  $\varepsilon_r$  is the relative permittivity of water.

It is assumed that we apply potentials,  $\phi_E$  (positive), and  $-\phi_E$ , to the anode and cathode, respectively, so that  $c_+$  and  $c_-$  are zero at the cathode ( $x = 0$ ) and the anode ( $x = w$ ). Since  $H^+$  and  $OH^-$ , in contrast, do not take part in the electrode reactions, respectively, at  $x = w$  and  $x = 0$ , their fluxes should be zero. Then the boundary conditions are

$$(c_+)_{x=0} = 0, (\partial c_- / \partial x)_{x=0} = 0, \phi_{x=0} = -\phi_E \quad (6)$$

$$(c_-)_{x=w} = 0, (\partial c_+ / \partial x)_{x=w} = 0, \phi_{x=w} = \phi_E \quad (7)$$

Equations (4) and (5) under the steady state are the same as the differential equations for Gouy-Chapman's theory except for the chemical reaction term.

Equation (4) is composed of three contributions; diffusion, electric migration and the chemical kinetics. Their magnitudes are estimated qualitatively here. We let the thickness of the diffusion layer be  $\Delta x$ , and the potential variation in this layer be  $\Delta \phi$ .

When voltage 1.5 V is applied to the cell with  $w = 50 \mu\text{m}$  including the thermodynamic potential (1.23 V for  $\text{H}_2\text{O} \leftrightarrow \text{O}_2$ ), the value  $\Delta\phi = (1.5 - 1.23)/2 = 0.13 \text{ V}$  is the net voltage applied to the one of two mass transport layers. If the thickness of the mass transport layer is close to that of the cell, the current densities controlled by diffusion and by the electric migration are, respectively, given by  $j_d = FDC^*/\Delta x = 0.02 \mu\text{A cm}^{-2}$  and  $j_m = (DF^2/RT) c^* \Delta\phi/\Delta x = 0.09 \mu\text{A cm}^{-2}$  for  $D = 10^{-5} \text{ cm}^2/\text{s}$ ,  $c^* = 10^{-7} \text{ M}$  ( $= \text{mol dm}^{-3}$ ). Since both are of the same order in magnitude, diffusion and electric migration contribute to the current in a similar way. If the reaction rates are fast enough to hold the equilibrium, Eq. (4) under the steady state is reduced to  $dc_{\pm}/dx \pm (F/RT)c_{\pm}d\phi/dx = \text{const}$ . These equations do not satisfy  $c_+c_- = K_{\text{H}_2\text{O}}$  except for  $c_{\pm} = c^*$ . The equilibrium condition does not hold and hence the kinetic term is inevitable.

It is difficult for us to obtain analytical solutions of Eq. (4) because not only of non-linearity of the chemical reaction term but also of actual non-linearity in  $c\phi$  [38-40]. We carry out numerical computation. The functional form of  $\phi$  is symmetric with respect to  $x = w/2$  owing to the common values of  $D$ , that is,  $\phi(x) + \phi(w-x) = 0$ . Replacing  $x$  by  $w-x$  in Eq. (4), and comparing the differential equations for  $c_{\pm}(x)$  with those for  $c_{\pm}(w-x)$ , we obtain  $c_+(x) = c_-(w-x)$ . By letting  $u = c_+/c^*$ ,  $z = x/w$  and  $f(x) = \phi(x)F/RT$ , Eq. (4) is reduced to

$$\frac{\partial u}{\partial t} = \frac{D}{w^2} \frac{\partial^2 u}{\partial z^2} + \frac{D}{w^2} \left( \frac{\partial u}{\partial z} \frac{\partial f}{\partial z} + u \frac{\partial f^2}{\partial z^2} \right) + c^* k_r (1-u(z)u(1-z))$$

When we take the finite difference,  $z_i = i\Delta z$  ( $0 \leq z \leq 1$ ,  $0 \leq i \leq N$ ),  $u(z_i) = u_i$  and  $f(z_i) = f_i$ , for integers  $i$  and  $N$ , the above equation becomes

$$u'_i = u_i + \bar{D}(u_{i+1} - 2u_i + u_{i-1}) + \bar{D}\{(u_{i+1} - u_{i-1})(f_{i+1} - f_{i-1})/4 + u_i(f_{i+1} - 2f_i + f_{i-1})\} + \bar{D} \frac{c^* k_r w^2 (\Delta z)^2}{D} (1 - u_i u_{N-i}) \quad (8)$$

where  $u_i$  and  $u'_i$  are  $u(z_i)$  at  $t$  and  $t+dt$ , respectively, and

$$\bar{D} = D\Delta t / (w\Delta z)^2$$

The finite difference form of Eq. (5) is

$$f_{i+1} - 2f_i + f_{i-1} = -\frac{F^2 w^2 (\Delta z)^2 c^*}{RT \varepsilon_0 \varepsilon_r} (u_i - u_{N-i}) \quad (9)$$

Boundary conditions (6) and (7) converted for Eq. (8) and (9) are given by

$$u_0 = 0, \quad u_{N-1} = u_{N+1}, \quad f_0 = -f_E, \quad f_N = f_E \quad (10)$$

We used known values of constants,  $k_r = 1.4 \times 10^{11} \text{ M}^{-1} \text{ s}^{-1}$ ,  $c^* = 10^{-7} \text{ M}$ ,  $D = 8.7 \times 10^{-5} \text{ cm}^2 \text{ s}^{-1}$ ,  $K = 1.8 \times 10^{-16} \text{ M}$  ( $=10^{-14}/55$ ) and  $\varepsilon_r = 78.5$ . Values of  $w$  were varied from  $3.3 \text{ } \mu\text{m}$  to  $34.0 \text{ } \mu\text{m}$ . Our computation technique of evaluating  $u_i$  and  $f_i$  from Eq. (8)-(10) was

(A) to set the initial values,  $u_i = 1$  and  $f_i = -f_E + 2if_E/N$  for  $1 \leq i \leq N$ ,

(B) to determine  $f_i$  for  $1 \leq i \leq N-1$  by means of Gauss-Jordan's method for Eq. (9) at known values of  $u_i$ ,

(C) to obtain  $u_i'$  at  $\Delta t$  for known values of  $f_i$  from Eq. (8) at  $D\Delta t / (w\Delta x)^2 = 0.48$ ,

(D) to determine  $f_i$  in Eq. (9) again by means of Gauss-Jordan's method for values of  $u_i$ , which were substituted for  $u_i'$  in step (C),

(E) to iterate processes (C) and (D) until  $\Sigma(u_i' - u_i)/N < 10^{-5}$ .

Even numbers of  $N$  sometimes made values  $f_i$  oscillated because of double uses of the identical term  $u_i u_{N-i}$  in Eq. (9), e.g.  $u_7 u_3$  and  $u_3 u_7$  for  $i=7$  and  $3$ ,  $N=10$ . We used odd numbers of  $N$  typically  $N = 101$  when  $2 \times 10^{-3} < c^* k_d w^2 / DN^2 < 0.22$ .

Figure 3 shows concentration profiles of  $\text{H}^+$  and  $\text{OH}^-$  for  $\phi_0 = 0.26 \text{ V}$  at  $w =$  (a)  $5 \text{ } \mu\text{m}$  and (b)  $10 \text{ } \mu\text{m}$ . The hydrogen ion is formed at the anode ( $x = w$ ) to increase  $c_+$  from  $c^*$  in the domain  $x > 0.2w$ . Although sharp variation of  $c_+$  at  $x = w$ , seems to be contradict to the boundary condition,  $(dc_+/dx)_{x=w}$ , we have confirmed the condition by magnifying the scale. With a decrease in  $w$ , distributions of both  $c_+$  and  $c_-$  become

uniform because of the large contribution of the chemical kinetics toward the equilibrium. The sum,  $c_+ + c_-$ , takes a minimum at the center of the cell, where the reaction rate is the smallest, as is intuitively predicted.

Figure 4 shows potential distributions in the cell for several values of  $\phi_E F/RT$ . The distributions are not a line, but is sigmoid or locally quadratic near the electrodes. A linear variation is predicted from Laplace's equation if  $c_+ = c_-$  in Eq. (5). The quadratic form results from  $c_+ \neq c_-$  near the electrodes. The variation increases with an increase in  $\phi_E$ , but is almost independent of  $w$ . The magnitude of the electric field takes a maximum at  $x = w/2$ , which is roughly proportional to  $\phi_E$ , as shown in the inset of Fig. 4. The slope is ca. twice larger than the average intensity of the electric field.

The current density at the cathode is given by  $j = -FJ_+$ , to which Eq. (3) is applied under the condition at the electrode,  $(c_+)_{x=0} = 0$ . Then we have

$$j/F = D(\partial c_+ / \partial x)_{x=0} = Dc^* (\partial u / \partial z)_{z=0} / w \approx Dc^* u_1 / (w\Delta z) \quad (11)$$

We express the dimensionless current density in terms of the thickness of the reaction layer [41],  $(D/k_d)^{1/2}$ , in order to discuss a relationship between  $j$  and  $w$ . Then it is rewritten as

$$\frac{j}{Fc^*} \sqrt{\frac{1}{Dk_d}} = \frac{u_1}{w\Delta z} \sqrt{\frac{D}{k_d}} \quad (12)$$

Figure 5 shows the plot of the dimensionless current density against  $w$ . The current density for  $\phi_E F/RT < 7$  (or  $\phi_E/2 < 90$  mV for (a) and (b)) decreases with an increase in  $w$ . The current density at  $w < 8 \mu\text{m}$  obeys the inverse proportional relation with  $w$  (dashed curve), which is the behavior of diffusion-controlled current in a thin layer cell. When  $\phi_E F/RT > 9$  for (c)-(g), the current density for small  $w$  increases with an increase  $w$  owing to the effect of electric migration. The current density for  $w > 25 \mu\text{m}$  approaches a constant, 1.5, at which the current is controlled by the reaction rate.

We obtain the ionic resistivity averaged over the cell by concentration distributions of  $H^+$  and  $OH^-$ . Letting the molar conductivity of  $H^+$  and  $OH^-$  be  $\lambda_+$  ( $= 0.0350 \text{ S m}^2 \text{ mol}^{-1}$ ) and  $\lambda_-$  ( $= 0.0199 \text{ S m}^2 \text{ mol}^{-1}$ ), respectively, and the average concentrations of  $H^+$  and  $OH^-$  be  $c_{+av}$  and  $c_{-av}$ , we obtain the expression for the conductivity as

$$\kappa = \lambda_+ c_{+av} + \lambda_- c_{-av} = \left( \lambda_+ \int_0^w c_+ dx + \lambda_- \int_0^w c_- dx \right) / w \quad (13)$$

Figure 6 shows the plot of the averaged resistivity ( $\rho = 1/\kappa$ ) against  $w$  for several values of  $\phi_E F/RT$ . The resistivity at large values of  $w$  agrees with the value for the uniform concentration,  $1/(\lambda_+ + \lambda_-)c^* = 0.18 \times 10^6 \text{ } \Omega\text{m} = 18 \text{ M}\Omega \text{ cm}$  (dashed line). With a decrease in  $w$ , the resistivity decreases because of increase in  $c_+$  and  $c_-$ . It also decreases with an increase in  $\phi_E F/RT$  by the same reason as above. Intuitively understandable plot is the resistance vs.  $w$ , as shown on the right ordinate in Fig. 6. The resistance per area of the cell is almost linear relation with  $w$ .

### 3.2 Voltammetry of pure water

Figure 7 shows a multi-cycled voltammogram of pure water at the parallel electrodes with  $w = 20 \text{ } \mu\text{m}$  in the cell of Fig. 2. A voltammogram at each scan overlapped with those at other scans when the potential width was less than 1.4 V (Fig. 7(A)). When the potential domain was more than 1.5 V, hysteresis was noticeable, and the maximum current increased with an increase in the number of scans (Fig. 7(B)). The increase in the current is ascribed to the redox cycle by the overlap of  $c_+$ -profiles with  $c_-$ -profiles (in Fig. 3). Poor reproducibility observed at voltage over 1.5 V seems to result from formation of gas bubbles, which is enhanced by the redox cycling. Voltammograms in negative voltage domains were symmetric with those in the positive domains with respect to the origin (current 0 and voltage 0). Therefore the electrode geometry and performance were confirmed to be symmetric.

Linear sweep voltammograms are shown for several values of  $w$  in Fig. 8(a)-(e). The current increases with a decrease in  $w$ , partly because the decrease in the solution resistance enhances the net voltage of water electrolysis. The  $w$ -dependence is consistent with the increase in or with the constant of the current density in Fig. 5 for  $\phi_E F/RT > 9$ .

Since the redox reaction of water is not followed by the Nernst equation as the boundary condition, the surface concentrations may not be controlled sufficiently with applied potentials. Thus the boundary condition,  $(c_+)_{x=0} = 0$ , is not satisfied well in the present experiment. It is expected that a Neumann condition (of controlling the current by the voltage) is valid rather than a Dirichlet condition (of the surface concentration by the Nernst equation). A typical equation of the former is Tafel equation, by which we can eliminate the electrode-kinetic overpotential from the observed voltage. The subtracted value should be close to the voltage relevant to the solution resistance. The curves for  $w > 1$  mm do not include contribution of solution resistance (in Fig. 8(g)). The plot of the logarithmic current against the voltage showed a line in the domain of 0.3 V, indicating that a Tafel type plot,  $\ln(I) = (\alpha F/RT)E_{\text{salt}} + b$ , is valid. The value of  $\alpha$  was  $0.17 \pm 0.01$  for both the anodic and the cathodic curves.

When the voltage applied in pure water contains the solution resistance,  $R_s$ , the current can be expressed by  $\ln(I) = (\alpha F/RT)E + b = (\alpha F/RT)(E_{\text{salt}} + IR_s) + b$ , where  $E - E_{\text{salt}} = IR_s$ . Values of  $E_{\text{salt}}$  and  $E$  at a common value of  $I$  were obtained, and those of  $E - E_{\text{salt}}$  were plotted against  $I$  for various values of the voltage in Fig. 9. The plots exhibit proportionality for  $40 \mu\text{m} < w < 100 \mu\text{m}$ . The proportionality was not valid for  $w > 0.1$  mm and  $I > 0.6 \mu\text{A}$  partly because of non-steady state voltammograms for  $w > 0.1$  mm and partly because of irreproducible voltammograms for  $I > 0.6 \mu\text{A}$ . The slope in Fig. 9 should be solution resistance, from which the resistivity was evaluated. The resistivity thus obtained was plotted against  $w$  in Fig. 10. It increases with an increase in  $w$ , as has been predicted theoretically in Fig. 6. It approaches to the resistivity value of the water

in the cell by the conductometer (dashed line). Although water just after the purification by the ultrapure water system showed 0.18 MΩ m, the water transferred in a glass vessel showed 0.04 MΩ m in air. When the pure water was further transferred into a polyethylene bottle and then a glass vessel, the resistivity was 0.02 MΩ m. The value decreased to 0.017 MΩ m after 30 min. Therefore the value of the dashed line in Fig. 10 is reasonable. A possible reason of the degrading the resistivity may be dissolution of carbon dioxide of air. The resistivity in the cell smaller than that in the bulk suggests  $c_+ + c_- > 2c^*$ . This condition holds when reaction (1) is far from the chemical equilibrium so that  $c_+c_- > K_{\text{CH}_2\text{O}}$ . In other word, pH values in the cell would depend on measurement times.

#### 4. Conclusions

Pure water can be electrolyzed in a thin layer cell when the distance of the electrodes is less than 100 μm. The conductance of water is provided by the products of H<sup>+</sup> and OH<sup>-</sup>, of which concentrations are satisfied with  $c_+ + c_- > 2 \times 10^{-7}$  M. This fact is contrary to the common knowledge that pure water is hardly electrolyzed. The conductivity enhances with a decrease in the inter-distance. The enhancement is an evidence of the electrochemical formation of H<sup>+</sup> and OH<sup>-</sup> which are far from the equilibrium.

The kinetically survived H<sup>+</sup> and OH<sup>-</sup> are controlled by diffusion, electric migration and the chemical reaction rates by similar quantities. Their concentration profiles were calculated by solving numerically the combination of Nernst-Planck equations, the continuum equation including the chemical reaction, and Poisson's equation under the steady-state. The sum of the concentration profiles are more than  $2 \times 10^{-7}$  M, as is deduced from experimental results of the conductivity. The numerical data of the present theoretical work include shortcomings due to the assumptions of a common

value of the diffusion coefficients and to use of the Dirichlet boundary conditions. Therefore they are not suitable for curve fitting to the experimental data.

## Acknowledgement

This work was financially supported by Grants-in-Aid for Scientific Research (Grants 22550072) from the Ministry of Education in Japan and a research fund by Permelec Electrode LTD.

## References

---

- [1] W. Ehrfeld, V. Hessel, H. Löwe, *Microreactors*, First edition, Wiley-VCH, Weinheim (2000).
- [2] C. Wille, R. Pfirmann, *Chemistry Today* (2004) 20
- [3] V. Hessel, H. Löwe, *Chem. Ingenieur Tech.* 74 (2002) 17.
- [4] H. Löwe, W. Ehrfeld, *Electrochim. Acta* 44 (1999) 3679.
- [5] P. Watts, S. J. Haswell, E. Pombo-Villar, *Chem. Eng. J.* 101 (2004) 23.
- [6] O. Scialdone, A. Galia, C. Guarisco, S.L. Mantia, *Chem. Eng. J.* 189–190 (2012) 229.
- [7] C.A. Paddon, G.J. Pritchard, T. Thiemann, F. Marken, *Electrochem. Commun.* 4 (2002) 825.
- [8] A. Attour, S. Rode, A. Ziogas, M. Matlosz, F. Lapique, *J. Appl. Electrochem.* 38 (2008) 339.
- [9] A. Attour, S. Rode, F. Lapique, A. Ziogas, M. Matlosz, *J. Electrochem. Soc.* 155 (2008) E201.
- [10] O. Scialdone, C. Guarisco, A. Galia, G. Filardo, G. Silvestri, C. Amatore, C. Sella, L. Thouin, *J. Electroanal. Chem.* 638 (2010) 293.
- [11] C. Belmont, H.H. Girault, *Electrochim. Acta*, 40 (1995) 2505.
- [12] S. Rode, S. Altmeyer, M. Matlosz, *J. Appl. Electrochem.* 34 (2004) 671.

- 
- [13] M. Sakairi, M. Yamada, T. Kikuchi, H. Takahashi, *Electrochim. Acta* 52 (2007) 6268.
- [14] A.J. Wain, R.G. Compton, R.L. Roux, S. Matthews, K. Yunus, A.C. Fisher, *J. Phys. Chem. B* 110 (2006) 26040.
- [15] A.J. Wain, R.G. Compton, *J. Electroanal. Chem.* 587 (2006) 203.
- [16] M.C. Henstridge, G.G. Wildgoose, R.G. Compton, *Langmuir* 26 (2010) 1340.
- [17] M.C. Henstridge, G.G. Wildgoose, R.G. Compton, *J. Phys. Chem. C* 113 (2009) 14285.
- [18] C. Amatore, M. Belotti, Y. Chen, E. Roy, C. Sella, L. Thouin, *J. Electroanal. Chem.* 573 (2004)333.
- [19] K. Bouzek, V. Jiricny, R. Kodym, J. Kristal, T. Bystron, *Electrochim. Acta* 55 (2010) 8172.
- [20] D.B. Baker, M.W. Verbrugge, J. Newman, *J. Electroanal. Chem.* 314 (1991) 23.
- [21] K.B. Oldham, *J. Electroanal. Chem.* 337 (1992) 91.
- [22] A. Amatore, B. Fosset, J. Bartelt, M.R. Deakin, R.M. Wightman, *J. Electroanal. Chem.* 256 (1988) 255.
- [23] K.B. Oldham, T.J. Cardwell, J.H. Santos, A.M. Bond, *J. Electroanal. Chem.* 430 (1997) 25.
- [24] A.M. Bond, M. Fleischmann, J. Robinson, *J. Electroanal. Chem.* 168 (1984) 299.
- [25] I. Montenegro, M.A. Queiros, J.L. Daschbach (Eds.), *Microelectrodes: Theory and Applications*, Kluwer, Dordrecht, 1991.
- [26] C. Lee, F. C. Anson, *J. Electroanal. Chem.* 323 (1992) 381.
- [27] K. Aoki, *Electroanalysis*, 5 (1993) 627.
- [28] J.C. Myland, K.B. Oldham, *J. Electroanal. Chem.*, 347 (1993) 49.
- [29] M. Ciszowska, Z. Stojek, *J. Electroanal. Chem.* 466 (1999) 129.
- [30] A. Jaworski, Z. Stojek, J.G. Osteryoung, *J. Electroanal. Chem.* 558 (2003) 141.
- [31] K. Aoki, A. Tokida, *Electrochim. Acta*, 45 (2000) 3483.

- 
- [32] C.A. Paddon, M. Atobe, T. Fuchigami, P. He, P. Watts, S.J. Haswell, G.J. Pritchard, S.D. Bull, F. Marken, *J. Appl. Electrochem.* 36 (2006) 617.
- [33] K. Aoki, M. Morita, O. Niwa, H. Tabei, *J. Electroanal. Chem.* 256 (1988) 269.
- [34] O. Niwa, M. Morita, H. Tabei, *Anal. Chem.* 62 (1990) 447.
- [35] V. A.T. Dam, W. Olthuis, A. van den Berg, *Analyst*, 132 (2007) 365.
- [36] S. Bose, T. Kuila, T.X.H. Nguyen, N.H. Kim, K.-t. Lau, J.H. Lee, *Prog. Polym. Sci.* 36 (2011) 813.
- [37] A. Goni-Urtiaga, D. Presvytes, K. Scott, *Intern. J. Hydrog. Engy.* 37 (2012) 3358.
- [38] J. Lu, D.-J. Li, L.-L. Zhang, Y.-X. Wang, *Electrochim. Acta* 53 (2007) 768.
- [39] D. Baker, M.W. Verbrugge, J. Newman, *J. Electroanal. Chem.* 314 (1991) 23.
- [40] B. Pillay, J. Newman, *J. Electrochem. Soc.* 140 (1993) 414.
- [41] P. Delahay, *New Instrumental Methods in Electrochemistry*, Interscience, New York, 1954, p.92-94.